frontiers | Frontiers in Ecology and Evolution

TYPE Original Research
PUBLISHED 19 February 2024
DOI 10.3389/fevo.2024.1336365

OPEN ACCESS

EDITED BY
Sylvain Charbonnier,
Muséum National d'Histoire Naturelle, France

REVIEWED BY
Lorenzo Lustri,
Université de Lausanne, Switzerland
Francesc Perez Peris,
The University of Iowa, United States

*CORRESPONDENCE
Dongjing Fu
djfu@nwu.edu.cn

†PRESENT ADDRESS
Stephen Pates,
Centre for Ecology and Conservation,
University of Exeter, Penryn Campus, Penryn,
Cornwall, United Kingdom

RECEIVED 10 November 2023
ACCEPTED 02 February 2024
PUBLISHED 19 February 2024

CITATION
Lin W, Pates S, Losso SR and Fu D (2024) Intraspecific variation of early Cambrian (stage 3) arthropod *Retifacies abnormalis* revealed by morphometric analyses. *Front. Ecol. Evol.* 12:1336365. doi: 10.3389/fevo.2024.1336365

Intraspecific variation of early Cambrian (stage 3) arthropod *Retifacies abnormalis* revealed by morphometric analyses

Weiliang Lin[1], Stephen Pates[2†], Sarah R. Losso[3] and Dongjing Fu[1*]

[1]State Key Laboratory of Continental Dynamics, Shaanxi Key Laboratory of Early Life and Environments, and Department of Geology, Northwest University, Xi'an, China, [2]Department of Zoology, University of Cambridge, Cambridge, United Kingdom, [3]Museum of Comparative Zoology and Department of Organismic and Evolutionary Biology, Harvard University, Cambridge, MA, United States

Retifacies abnormalis is a large artiopodan euarthropod known only from the famous fossil deposits of the Chengjiang biota, China (Cambrian Series 2, Stage 3). It is well known for its pronounced reticulated ornamentation that covers the entire dorsal surface of the exoskeleton. Here 109 new specimens of *R. abnormalis* from multiple deposits are reported. Some larger specimens display a distinct carapace ornamentation to what was previously known. By qualitatively separating specimens into two groups ('Morph A', 'Morph B') and analyzing the shape of the body, pygidium, and shape of the polygons in the reticulation, using linear and geometric morphometrics and elliptical Fourier analysis, the two morphs are shown to overlap in morphospace and display similar length:width ratios of body parts, rather than form two distinct clusters. The differences are interpreted as intraspecific rather than as diagnosing two species. As Morph B are only found in larger size classes, *R. abnormalis* ornamentation differences are interpreted to have developed during ontogeny, but are not thought to represent sexual dimorphs.

KEYWORDS

Cambrian, Chengjiang biota, arthropoda, *Retifacies*, intraspecific variation, morphometric analysis

1 Introduction

Artiopoda are a diverse group of euarthropods, and common components of early Palaeozoic marine communities (e.g. Ortega-Hernández et al., 2013). This group comprises trilobites with calcite exoskeletons and their non-biomineralized relatives, united by possession of a headshield anterior to a dorso-ventrally flattened exoskeleton concealing a series of broadly homonomous biramous appendages (Stein and Selden, 2012; Ortega-

Hernández et al., 2013; Giribet and Edgecombe, 2019). These taxa possess uniramous antennae and at least three pairs of biramous limbs (e.g. Ortega-Hernández et al., 2013). Although traditionally considered to have homonomous appendages, recent work has shown some artiopodans to displaying impressive limb specialization (e.g. Stein et al., 2013; Chen et al., 2019; Schmidt et al., 2022). Non-trilobite artiopodans are known exclusively from deposits preserving soft-tissues because of the lack of biomineralized tissues, such as the Chengjiang (China), Burgess Shale (Canada), Emu Bay Shale (Australia), and Great Basin (USA) (e.g. Hou and Strom, 1997; Stein, 2011; Paterson et al., 2012; Stein and Selden, 2012; Ortega-Hernández et al., 2013; Hou et al., 2017; Du et al., 2019; Lerosey-Aubril and Ortega-Hernández, 2019; Lerosey-Aubril et al., 2020; Schmidt et al., 2022; Zhu et al., 2023).

Retifacies Hou et al., 1989 is a large artiopodan euarthropod known only from the Chengjiang biota (Cambrian Series 2, Stage 3) (e.g. Hou et al., 1989; Zhang et al., 2022). It is closely related to *Pycmaclypeatus daziensis* Zhang et al. (2000), either in an early diverging clade within Artiopoda or in a more derived position within the trilobitomorphs (Schmidt et al., 2022). Originally two species were described from the Chengjiang (Hou et al., 1989; Luo et al., 1997). Luo et al. (1997) suggested the species *Retifacies longispinus* Luo et al., 1997 based on the presence of a curved caudal spine that projects out from underneath the pygidium, but they later considered *R. longispinus* as a synonym of *R. abnormalis*. *R. longispinus* Luo & Hu is now considered a junior synonym of the type species *R. abnormalis* Hou et al., 1989 (Hou et al., 2017; Zhang et al., 2022). Therefore, *R. abnormalis* remains the only known species of this monospecific genus. *Retifacies* has a broadly elliptical outline, comprising a semicircular cephalon, an articulating thorax composed of 10 tergites, and a pygidium anterior to a multisegmented tailspine (e.g. Hou et al., 1989; Zhang et al., 2022). Ventrally, the appendicular morphology is well known, comprising four uniramous cephalic post-antennal appendages followed by seven biramous limbs distributed across the thorax and pygidium (Zhang et al., 2022). The dorsal surface of the exoskeleton displays a pronounced reticulated ornamentation (Figures 1, 2) (Hou et al., 1989).

Retifacies is one of the rarest taxa in Chengjiang biota, accounting for no more than 0.1% in specimen abundance (Zhao et al., 2010). Thirty years of excavation of the Chengjiang biota by LELE (Shaanxi Key Laboratory of Early Life and Environments, Northwest University, Xian, China) has led to a discovery of 109 specimens of *Retifacies*, which allow to the further analysis and reinterpretation of these specimens. These specimens are of various sizes and display different patterns of reticulation on the exoskeleton which has not previously been investigated, and may represent inter- or intraspecific variation.

Species is the basic unit of classification and a taxonomic rank of an organism (Smith, 1998; De Queiroz, 2007). For paleontologists, morphology differences are the ruler that divides species boundaries (De Queiroz, 2007). We define the difference with the empirical basis and observation of character states. But it is hard to describe exactly how much difference is needed to distinguish two species. Within artiopodans, the trilobite *Dikelocephalus minnesotensis* Owen, 1852 provides a comprehensive example of how interspecific differences can be misinterpreted as intraspecific, with up to 26 species erected in 1930 later synonymized to one (Labandeira and Hughes, 1994; Hughes and Labandeira, 1995). Documentation and quantification of intraspecific variation, which can result from changes during ontogeny, sexual dimorphism, responses to environmental factors leading to phenotypic differences are critical for stable systematic schemes (Fusco and Minelli, 2010). Determining that such variation is continuous, rather than discrete, is critical for inferring that it is intraspecific rather than of broader taxonomic significance (e.g. Labandeira and Hughes, 1994; Esteve and Zamora, 2014). However, this can be complicated by different post-embryonic growth modes in euarthropods. Broadly speaking, euarthropods can be separated into three main growth modes: anamorphic, where segments are added continuously; epimorphic, where no segments are added; and hemianamorphic, where segments are added up to a specific growth stage, after which no further segments are added (e.g. Hughes et al., 2006; Minelli and Fusco, 2013). While morphological changes during ontogeny can occur in animals following any of these three growth modes, anamorphic and hemianamorphic growth modes introduce an additional likelihood for incorrectly interpreting intraspecific variation and interspecific. This is because the addition of segments can co-occur with other changes to the morphology, such as a reduction in ornamentation, increase in effacement, or changes to the lengths of spines or other features. In this study we utilize morphometrical analysis on the outline of the pygidium of *Retifacies abnormalis* individuals, as well as the polygon ornamentation of the dorsal exoskeleton, to quantify morphological variation within our sample. Our quantitative results illustrate these features represent possible cases of developmental variation, most likely due to the aging processes of the population, rather than provide support for splitting into two discrete species.

2 Materials and methods

2.1 Material and observation

The material studied comprises 109 specimens of *Retifacies abnormalis*, which are housed in the Museum of Northwest University, China. The collection comes from three localities (Jianshan, Erjie, and Sanjiezi), identified by the prefix "JS", "EJ" and "SJZ" respectively of the Chengjiang Lagerstätte.

Specimens are from the Yu'anshan Member of the Helinpu Formation, *Eoredlichia* Zone, Stage 3, Series 2 of the Cambrian in Yunnan, China (Zhang et al., 2001, 2008; Fu et al., 2011). Chengjiang Biota inhabited a storm-flood-dominated delta with dark, organic-rich mudstone of the hemipelagic deposits (Saleh et al., 2022). Most the specimens were preserved with the exoskeleton in dorsal view due to the flattened organization of the body. Specimens were examined and photographed illuminated by an LED lamp at a low angle to the sample plane in order to enhance the relief of these highly compacted fossils. Morphological descriptive terms follow those used in previous studies about *Retifacies* (Hou and Strom, 1997; Hou et al., 2004, 2017; Zhang et al., 2022).

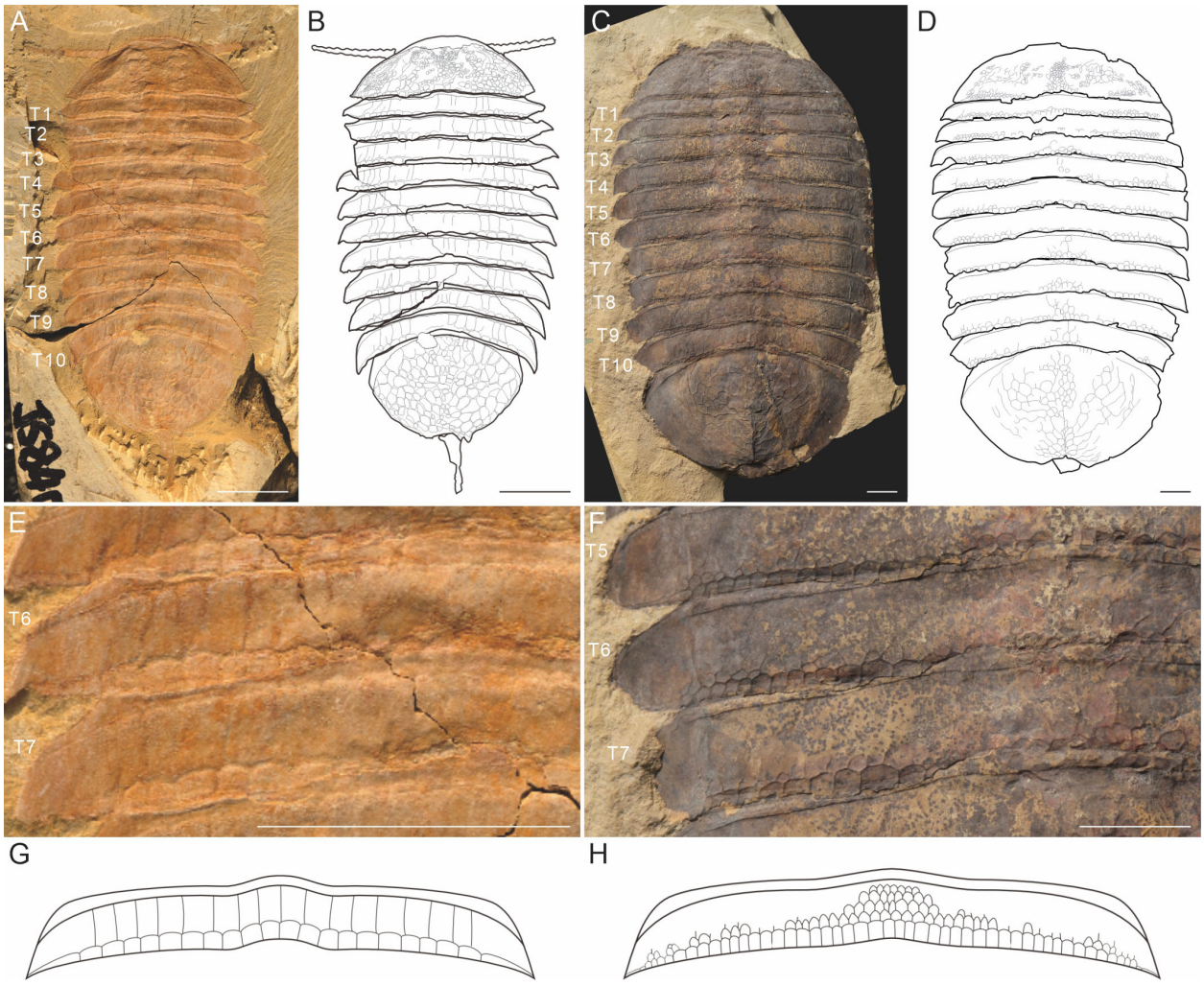

FIGURE 1
The gross morphology of *Retifacies abnormalis* from the Cambrian Chengjiang biota, showing the differences of the reticulated ornamentation of the dorsal exoskeleton in two morphs. **(A, B)** Morph A, representing by the specimen JS-840, and the line drawing; **(C, D)** Morph B, representing by the specimen XDBZ-084, and the line drawing; **(E, F)** magnification of the trunk tergite 5 to 7 (T5-T7) in *A* and *B*, showing the differences in the arrangement of the reticulated ornamentation; **(G)** the reconstruction of the reticulated ornamentation of one trunk tergite in Morph A, note that the two rows arranged pattern, the anterior one is rectangular-shaped and extends to the anterior margin of the tergite; **(H)** reconstruction of the ornamentation pattern of one trunk tergite in Morph B, which defined by the axial region with densely distributed rectangular ornamentation, and the off axial region without ornamentation at the anterior region; note that the reduction and loosely arrangement of the anterior row of the polygon ornaments.

2.2 Measurements and morphometric analysis

Of the collection of 109 specimens reported here, only complete specimens preserved parallel to the bedding plane in dorsoventral aspect, and sufficiently well-preserved, were measured and used in the morphometric analysis (79 specimens). Specimens were separated in to two categories, labelled 'Morph A' and 'Morph B' based on differences in the reticulation (more details in Results below). The violin plot (i.e., box plots made of Kernel density distributions, see Figure 3) of the body length was performed with Power BI visual tool Violin Plot 1.3.0 (Ma et al., 2023). Measurements of the length (sag.) and width (trans.) of the cephalon, thorax, pygidium and the total exoskeleton of two morphs were compared in raw units (mm) and log form (Figure 4). The width of the thorax refers to the widest of the thorax at the fourth and fifth tergite. Morph A is abundant, represented by 29 complete specimens, and 72 incomplete specimens (37 samples for cephalon, 35 samples for thorax, 57 samples for pygidium). Fewer Morph B specimens were recognized (eight), all of which were measured. For the incomplete specimens among these samples, we estimated the total length of the exoskeleton based on measurable data, such as width, pygidium length (ratio conversion with the average proportion measured from the complete specimens). This was calculated from data of complete Morph B specimens, using the relative lengths of the total body, cephalon, thorax and pygidium. We used the ratio of length/width as a proxy for cephalic, thoracic and pygidium shape. Regression analysis was performed in Microsoft Excel (see Figure 4).

FIGURE 2
The dorsal view of the two morphogroups. **(A-D)** specimens representing Morph A; **(A)** SJZ-B02-001, the rectangular ornamentation preserved in highly relief; **(B)** SJZ-B01-015, ornamentation depicted by the dark lines, pygidium completely decorated by polygons both in axial and side region; **(C-D)** details of box in *A* and *B*, showing the two rows of the polygon ornamentations, note that the anterior row of the rectangular-shaped ornaments reaches to posterior margin of articulating ridge; **(E-I)** specimens representing Morph B, showing the rectangular ornamentation of the dorsal exoskeleton; **(E)** specimen JS822, a complete specimen showing the outline of the dorsal exoskeleton, the axial region of the trunk with dense rectangular ornamentation, and the labrum; **(F)** magnification of box in *E*, showing the off axial region of the tergite, the posterior row of polygon ornaments is similar to that of Morph A, while the anterior region of the tergite is relative smooth; **(G)** part of specimen SJZ-B14-019, note that the central axis of the trunk tergite in Morph B is featured by densely distributed rectangular ornamentation; and shows a very clear pattern in the off axial region: the anterior row of the polygon ornaments is reduced or loosely arranged, causing the anterior region of the tergite smoothly; **(H)** the counterpart of specimen SJZ-B14-019, the central axis of the trunk in Morph B is characterized by the densely distributed polygon ornaments; **(I)** magnification of the box in *G*, the detail of the cephalic shield showing the rectangular ornamentation of Morph B might be denser than that of Morph A; note that paired ventral lateral eyes (ve, see arrow) located close to the anterior margin of the head shield. Scale bar: 10 mm.

The further comparison of the two morphs were carried on the shape of the pygidium. A total of 25 intact specimens without deformation were selected for geometric morphometric analyses, 23 Morph A, and 2 Morph B. All selected specimens were imaged in dorsal view, and aligned. A total of 8 landmarks points were digitized (Table 1) with the software tpsDig v2.16 (Rohlf, 2010). Landmark 1 is at anteriormost point of pygidium along midline and other seven landmarks are established clockwise at the maximum bending points along the marginal rim of the pygidium, two of them are located on the posterior spines (Figure 5). The software tpsUtil v1.44 was applied to transfer curves to landmarks. A generalized Procrustes analysis (GPA) was performed using tpsRelw v1.49.

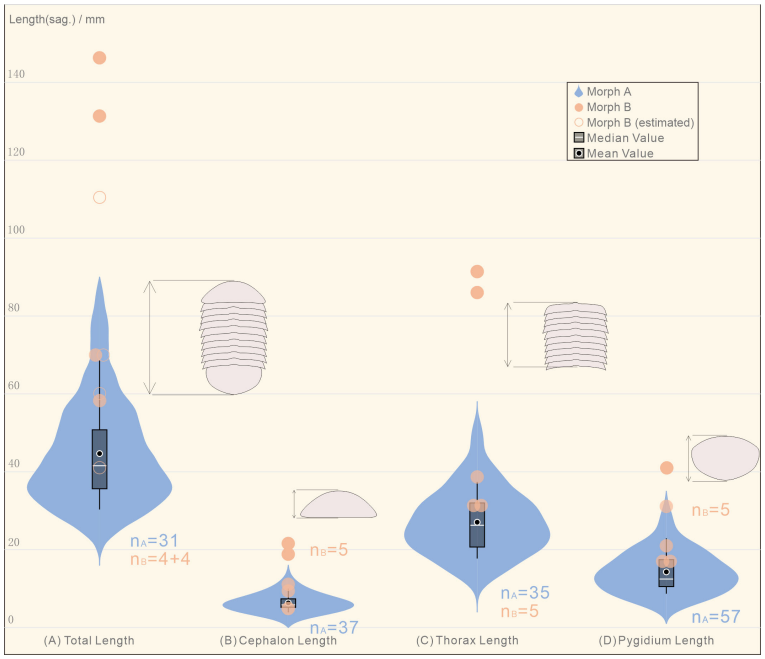

FIGURE 3
Violin plot showing the distribution of the different parts of the body length in the collection of *Retifacies abnormalis* specimens. **(A)** Morph A, the total length of the most specimens locates at 28-72 mm, the median/mean value is ca. 45 mm; Morph B, all of the four complete specimens are larger than 59 mm, the largest one is reaching up to 146 mm, the mean value is ca. 91 mm; **(B)** the cephalic length of Morph A is concentrated in the range of 4-12 mm, the mean value is ca. 6 mm, while that of the Morph B is in the range of 6-22 mm, the mean value is ca. 13 mm; **(C)** the thoracic length refers to the total length of the ten tergites, the mean value of Morph A is ca. 27 mm, while the thoracic length of Morph B in five complete specimens is more than 33 mm; **(D)** the pygidium length of Morph A ranges from 7 to 27 mm; the length of the most specimens locate around 13 mm, which are shorter than that of all the Morph B specimens.

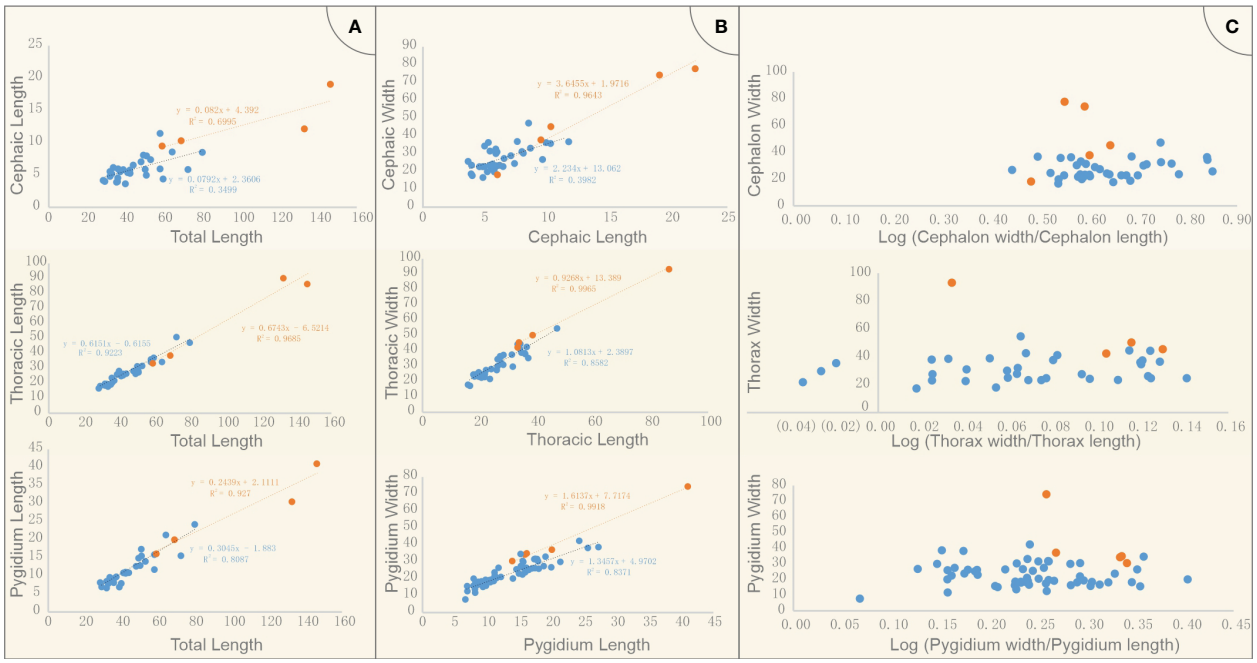

FIGURE 4
Measurements of cephalon, thorax, pygidium and the total length of *Retifacies abnormalis* specimens in two morphs. **(A)** cephalic length, thoracic length, pygidium length vs body length; two morphs were compared in raw units; **(B)** cephalic, thoracic, pygidium width vs length; two morphs were compared in raw units; **(C)** Morphometric analyses of *Retifacies abnormalis* two morphs in log form; ratio of width/length as a proxy for cephalic, thoracic and pygidium shape. Blue and orange present Morph A and Morph B respectively.

TABLE 1 Definitions of landmarks used in analysis (see Figure 5).

Landmark N	Positon of Landmark N
Landmark 1	Anteriormost point of pygidium along midline
Landmark 2	Inflection point between landmark 1 and landmark 3
Landmark 3	Point furthest right on pygidium
Landmark 4	Inflection point between landmark 3 and landmark 5
Landmark 5	Posteriormost point of pygidium along midline
Landmark 6	Inflection point between landmark 5 and landmark 7
Landmark 7	Point furthest left on pygidium
Landmark 8	Inflection point between landmark 7 and landmark 1

Relative warp analysis (RWA) was carried out to analysis of within-population morphometric variation based on landmark data (Rohlf, 1993). This is an well-established method in geometric morphometrics for describing and discriminating between organisms (Requieron et al., 2012). The morphometric data was plotted by PAST v3.12 (Hammer, 2001).

Outline analysis was used to compare the shapes of polygons in the reticulation of morphs A and B. This analysis was focused on the posterior row of the ornament polygon on the fourth tergite, which are similar in morphology between Morph A and Morph B. Polygons were converted to black silhouettes on white backgrounds using Inkscape, converted to.jpgs and imported into the R environment using the Momocs package (Bonhomme et al., 2014;"R Core"Team et al., 2022). These were then converted to outlines, sampled at a 64 points resolution, scaled, centered, and subjected to elliptical Fourier analysis. Results were visualized using principal components analysis, and a Linear discriminant analysis was then used to determine whether Morph A and Morph B could be distinguished by the shape of polygons making up the reticulation patterns.

3 Results

3.1 Description of the dorsal exoskeleton of *Retifacies abnormalis*, with the difference of the reticulated ornamentation in Morph A and Morph B

Individuals varied in body size, from 28 mm to 146 mm in length, representing different growth stages. The dorsal side of the exoskeleton is heavily ornamented with a reticulated pattern consisting mostly of pentagon and hexagon polygons. We recognized two different morph groups (Morph A and Morph B) in our collection, defined by the different pattern of ornamentation (Figure 1).

The following features were used to distinguish Morph A and Morph B in our collection: 1) the trunk has a poorly defined raised axial region without furrows in both morphs, however the arrangement of reticulated ornamentation is different. The axial region of Morph A shows the same pattern of ornamentation to the off axial region (Figures 2C, D), while the axial region of Morph B bears polygons which are smaller in size and more densely distributed (Figure 2G); 2) there are two rows of the ornament polygon in both morphs, in which the posterior row shows similar in outlines (Figure 1); In Morph A, the anterior one is rectangular-shaped and extends to the anterior margin of the tergite (Figure 1E); In Morph B, the anterior row of the polygon ornaments is reduced or loosely arranged (Figure 1F);

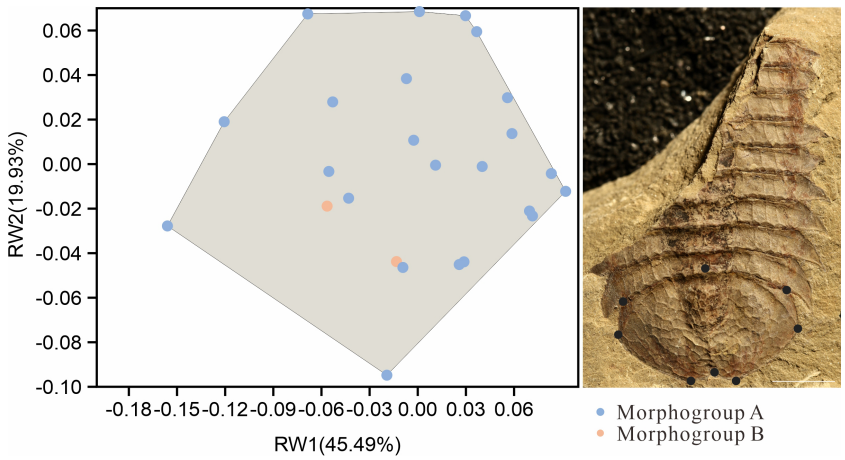

FIGURE 5
Landmark-based geometric morphometric analysis of the outline of the pygidium in two morphs of *Retifacies abnormalis*. Specimens preserved in dorsal view, with 8 landmarks along the pygidium outline. Blue point representing samples of Morph A, orange points representing Morph B; note that the orange points fall within the shadow formed by the blue points, indicating that there are no clear difference between Morph A and B in outline of pygidium. Scale bar: 10 mm.

3) the margin of the pygidium is smooth, without any ornamentation in Morph B (Figure 1C); 4) the reticulated ornamentation of the head shield arranged more densely in Morph B (Figures 2H, I).These differences are summarized in Table 2.

3.2 Morphometric analyses of the outline of the dorsal exoskeleton in two morphogroups of *Retifacies abnormalis*

To determine whether there are significant morphological differences between the two morphogroups, we used the violin plot showing the distribution of the different parts of the body length of all the complete specimens. The total length of the specimens in Morph A arranges from 28 mm to 80 mm, the median/mean value is ca. 45 mm; while the four complete specimens are larger than 59 mm, the largest one is 146 mm, the mean value is ca. 91 mm (Figure 3). The cephalic length of Morph A is concentrated in the range of 4-12 mm, while that of the Morph B occupies a wider space, from 6 mm to 22 mm. The thoracic length refers to the total length of the ten tergites, five complete specimens of Morph B could reach to 86 mm long (mean value ca. 48 mm), whereas specimens of Morph A are only 47mm (mean value ca. 27 mm). A similar situation occurs in the measurement of the pygidium length, with Morph B is larger than Morph A. For visual comparison, the data were made into scatter plots and regression were fitted (Figures 4A, B). The scattered points representing the cephalon shows a certain degree of dispersion, while thorax and pygidium data are relatively clustered. Comparison of cephalic, thoracic, pygidial and total-length measurements and regression analyses show that Morph B specimens are large compared to the whole population, but show similar ratios between these measurements as Morph A specimens. We also used the logarithmic function to explore the differences between the two morphs. The results of no cluster separation exclude the possibility for splitting into two discrete species (Figure 4C).

TABLE 2 Summary of criteria used to separate material into Morph A and Morph B.

	Morph A	Morph B
Distribution of thoracic ornamentation on axial region and off-axial region	Same ornamentation on both axial region and off-axial region	Polygons are smaller and more densely distributed on axial region Polygons do not compeletely cover the anterior margin of tergite on off-axial region
Shape of anterior row(s) of thoracic polygonal ornamentation	Rectangular shaped polygons extend to anterior margin of tergite	Reduced or loosely arranged nearly square polygonal ornamentation
Distribution of pygidium ornamentation on anterior margin	Displays ornamentation	Smooth, lacking ornamentation
Distribution of ornamentation on the head shield	Less dense	More dense

Geometric morphometrics analysis was used to determine whether there are morphological differences in the pygidium of the two morphs (Figure 5). 25 complete and undeformed pygidia (Selected from 77 specimens with pygidia) were used for relative warp analysis (RWA) (Bookstein, 1989; Bookstein et al., 1991). The blue points represent specimens assigned to Morph A (23 specimens) and the red points represent specimens with assigned to Morph B (2 specimens) (Figure 5). The first identified warp score (RW1) accounts for 45.49% of the total morphological variance, followed by 19.93% for RW2. The first two RWs jointly account for 65.83% of the total variance. RW1 and RW2 scores mainly concern the radio of length (sag.) and width (trans.) of pygidium. A larger H/W (height/width) value will get a higher RW1 score and a lower RW2. A smaller H/W (height/width) value, results in a lower RW1 and a bigger RW2 score. Results show no variations in shapes between specimens with different ornamentation patterns (Figure 5). The relative warp analysis indicates that the pygidium shape of the two morphs overlaps, and that pygidium shape cannot be used to discriminate two species.

3.3 Morphometric analyses of ornament polygons in two morphogroups of *Retifacies abnormalis*

Morphometric analysis comparing the outline shapes of the posterior row of ornament polygons of specimens assigned as morphogroups A and B in R. abnormalis did not discriminate two distinct groups. The result of visualization in PCA space shows that while the extremes of the polygons differ between the morphs, occupation of the morphospace shows broad overlap between morph A and B (Figure 6A). The distributions of morphs A and B across PC2 and PC3 are broadly similar, however more Morph A specimens tend to have more negative PC1 values, and more Morph B specimens more positive values (Figures 6A, B). Linear Discriminant Analysis could also not separate the groups (Figure 6C). These results show overlapping distributions of the two morphs (Figures 6A-C), with some differences in the density in negative/positive areas of PC1.

4 Discussion

The pronounced reticulated ornamentation on the dorsal exoskeleton in *Retifacies abnormalis* (Figure 7) might be interpreted as a feature compromising between weight and strength of the exoskeleton, as suggested for *Tuzoia* Walcott, 1912 (Vannier et al., 2007). In other arthropods similar reticulation patterns have been suggested to have performed a hydrodynamic function in facilitating locomotion or retarding sinking (Vannier and Chen, 2000; Vannier et al., 2007), though for a dorso-ventrally flattened benthic arthropod such as *Retifacies* the latter seems an unlikely function.

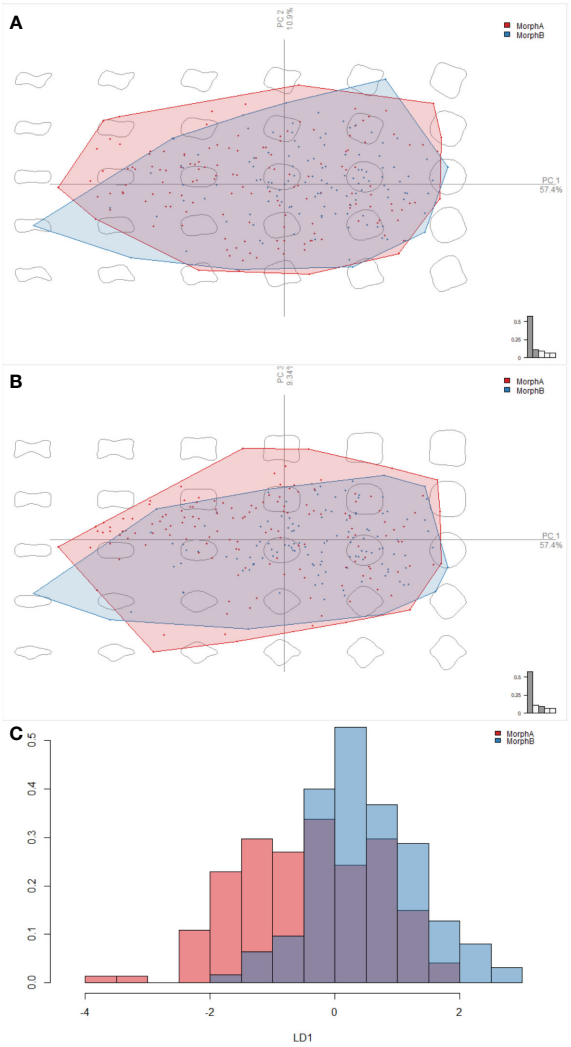

FIGURE 6
Results of the elliptical Fourier analyses, comparing the outline shapes of the posterior row of ornament polygons of Morphs A and B in *Retifacies abnormalis*. **(A, B)** a visualisation in PCA space, showing overlap between Morphs A and B along PC1, PC2, and PC3; **(C)** the linear discriminant analysis, showing the overlap between the shapes of Morphs A and B along the linear discriminant, and thus that the two cannot be clearly separated.

FIGURE 7
Reconstructions of endmembers, Morph A and Morph B, showing the morphological differences of the polygon ornamentation of the dorsal exoskeleton.

Variation in the reticulation of *Retifacies abnormalis* could indicate interspecific variation within a genus (e.g. Crônier, 2010; Mayers et al., 2019; Lei et al., 2023), change during ontogeny (e.g. Esteve, 2012; Fu et al., 2014), sexual dimorphism (Fu et al., 2014), a response to external environmental factors (Jackson and Budd, 2017), or a combination of these factors. Different patterns in the morphometric size analyses are expected for each of these possibilities, allowing for comparison between them.

If the two morphs represent distinct, but closely related species, non-overlapping patterns in the reticulation, outline morphology, and distinct morphological characters would be expected. The overlap in morphospace of both polygon shape in the reticulation and shape of the pygidium (Figures 5, 6) support the interpretation that these specimens represent a single species with intraspecific variation, rather than two separate species. Morphometric analyses on other artiopodans, such as the trilobite *Eccaparadoxides* Šnajdr, 1957, have indicated that some qualitative differences in morphology can be shown to represent a continuum, leading to material previously thought to represent multiple species being recognized as a single taxon (e.g. Esteve, 2012). Similarly, the two morphs most likely do not represent a result of phenotypic plasticity in response to different environments, since the two morph specimens are found across three localities.

The reticulation pattern assigned to Morph B is restricted to larger specimens (at least 59 mm length), while the Morph A pattern is found across a broad range of specimen sizes (28 - 80 mm). This indicates an ontogenetic change that takes place in some individuals, when they reach ~55 mm long, involving a gradual shift in the polygon pattern – the reticulation pattern tends to no longer cover the entire exoskeleton. This change can be interpreted as gradual rather than abrupt as the polygon shapes of specimens attributed to Morph A and Morph B overlap – they do not form two distinct clusters and cannot be separated by Linear discriminant analysis. Rectangular polygons reduced in size, coverage, and altered in shape to become squarer in some larger specimens. Crucially, some large specimens remain as Morph A, with prominent rectangular polygonal ornament, showing gradually changes of the ornamentation of the two morphogroups.

Multiple explanations can be offered for these ontogenetic changes. For example, sculpture patterns change throughout the

lifecycle of trilobites, with spines becoming less prominent (Hopkins and Webster, 2009), but might also reflect the onset of sexual maturity (e.g. Cederström et al., 2011). The continuum of polygon shapes across Morph A and B (Figure 6) suggests that this change might have taken place over multiple growth stages, rather than occurring in a single molt as in other secondary sexual characters (Drago et al., 2011; Akkari et al., 2014). Sexual dimorphism is particularly difficult to recognize in the fossil record because of the challenges associated with demonstrating that the morphs represents a single species with distinct characters between male and female. Males of the trilobite *Olenoides serratus* Röminger, 1887 have been shown to display specialized claspers used during mating (Losso and Ortega-Hernández, 2022). Size differences within a species have also been suggested to represent sexual dimorphism (Hu, 1971; but see Hughes and Fortey, 1995). In other trilobites, inflated glabellar fields have been interpreted as brood pouches, and as an indicator for sexual dimorphism (Fortey and Hughes, 1998) while in raphiorid trilobites medial cephalic protuberances have been suggested to be the result of sexual dimorphism (Knell and Fortey, 2005). The ornamentation would not have played a primary role such as clasping or brood care in *Retifacies*. Similarly, reticulation cannot be argued to have played a secondary sexual role such as display, as it reduced in Morph B, rather than increasing as expected for secondary sexual characters such as the protuberances of raphiorids (Knell and Fortey, 2005).

Our study demonstrated that the sculpture covering and the body size was negatively correlated in *Retifacies*, that is the larger individuals bearing the less decoration. The ontogenetic decreases in the decoration also observed in some euarthropods, for example, majoid crabs (Hultgren and Stachowicz, 2009). Decrease in reticulation pattern may be a resource-saving strategy of *Retifacies*, because of the lowered adaptive value of dense decoration for larger individuals that have reached a size refuge from predation (Berke and Woodin, 2008; Hopkins and Webster, 2009), or a reduction in the need for a carapace that combines lightness and weight balance the reticulation pattern structure could provided.

Data availability statement

The original contributions presented in the study are included in the article/Supplementary Material, further inquiries can be directed to the corresponding author.

Author contributions

WL: Writing – original draft, Writing – review & editing, Data curation. SP: Writing – original draft, Writing – review & editing, Software, Visualization. SL: Writing – review & editing, Formal analysis, Investigation. DF: Writing – original draft, Writing – review & editing, Project administration, Resources.

Funding

The author(s) declare financial support was received for the research, authorship, and/or publication of this article. This research was supported by the National Natural Science Foundation of China (41930319), the National Key Research and Development Program of China (2023YFF0803601), 111 Project (D17013), Natural Science Basic Research Plan of Shaanxi Province (2022JC-DW5-01), and a Herchel Smith Postdoctoral Fellowship (University of Cambridge) to Stephen Pates.

Conflict of interest

The authors declare that the research was conducted in the absence of any commercial or financial relationships that could be construed as a potential conflict of interest.

Publisher's note

Supplementary material

The Supplementary Material for this article can be found online at: https://www.frontiersin.org/articles/10.3389/fevo.2024.1336365/full#supplementary-material

References

Akkari, N., Enghoff, H., and Minelli, A. (2014). Segmentation of the millipede trunk as suggested by a homeotic mutant with six extra pairs of gonopods. *Front. Zool.* 11, 1–22. doi: 10.1186/1742-9994-11-6

Berke, S. K., and Woodin, S. A. (2008). Energetic costs, ontogenetic shifts and sexual dimorphism in majoid decoration. *Funct. Ecol.* 22, 1125–1133. doi: 10.1111/j.1365-2435.2008.01469.x

Bonhomme, V., Picq, S., Gaucherel, C., and Claude, J. (2014). Momocs: outline analysis using R. *J. Stat. Software.* 56, 1–24. doi: 10.18637/jss.v056.i13

Bookstein, F. L. (1989). Principal warps: Thin-plate splines and the decomposition of deformations. *IEEE Trans. Pattern Anal. Mach. Intell.* 11, 567–585. doi: 10.1109/34.24792

Bookstein, F. L., Grayson, B., Cutting, C. B., Kim, H. C., and McCarthy, J. G. (1991). Landmarks in three dimensions: reconstruction from cephalograms versus direct observation. *Am. J. Orthodontics. Dentofacial. Orthopedics.* 100, 133–140. doi: 10.1016/S0889-5406(05)81520-3

Cederström, P., Ahlberg, P., Nilsson, C. H., Ahlgren, J., and Eriksson, M. E. (2011). Moulting, ontogeny and sexual dimorphism in the Cambrian ptychopariid trilobite Strenuaeva inflata from the northern Swedish Caledonides. *Palaeontology* 54, 685–703. doi: 10.1111/j.1475-4983.2010.01021.x

Chen, X. H, Ortega-Hernández, J., Wolfe, J. M., Zhai, D. Y., Hou, X. G., Chen, A. L., et al. (2019). The appendicular morphology of Sinoburius lunaris and the evolution of

the artiopodan clade Xandarellida (Euarthropoda, early Cambrian) from South China. *BMC Evol. Biol.* 19 (1), 1-20. doi: 10.1186/s12862-019-1491-3

Crônier, C. (2010). Varied development of trunk segmentation in three related Upper Devonian phacopine trilobites. *Historical. Biol.* 22, 341–347. doi: 10.1080/08912960903548712

De Queiroz, K. (2007). Species concepts and species delimitation. *Syst. Biol.* 56, 879–886. doi: 10.1080/10635150701701083

Drago, L., Fusco, G., Garollo, E., and Minelli, A. (2011). Structural aspects of leg-to-gonopod metamorphosis in male helminthomorph millipedes (Diplopoda). *Front. Zool.* 8, 1–16. doi: 10.1186/1742-9994-8-19

Du, K. S., Ortega-Hernández, J., Yang, J., and Zhang, X. G. (2019). A soft-bodied euarthropod from the early Cambrian Xiaoshiba Lagerstätte of China supports a new clade of basal artiopodans with dorsal ecdysial sutures. *Cladistics* 35, 269–281. doi: 10.1111/cla.12344

Esteve, J. (2012). Intraspecific variability in paradoxidid trilobites from the Purujosa trilobite assemblage (middle Cambrian, northeast Spain). *Acta Palaeontol. Polonica.* 59, 215–240. doi: 10.4202/app.2012.0006

Esteve, J., and Zamora, S. (2014). Enrolled agnostids from Cambrian of Spain provide new insights about the mode of life in these forms. *Bull. Geosci.* 89, 283–291. doi: 10.3140/bull.geosci.1416

Fortey, R. A., and Hughes, N. C. (1998). Brood pouches in trilobites. *J. Paleontol.* 72, 638–649. doi: 10.1017/S0022336000040361

Fu, D. J., Zhang, X. L., Budd, G. E., Liu, W., and Pan, X. Y. (2014). Ontogeny and dimorphism of Isoxys auritus (Arthropoda) from the early Cambrian Chengjiang biota, South China. *Gondwana. Res.* 25, 975–982. doi: 10.1016/j.gr.2013.06.007

Fu, D. J., Zhang, X. L., and Shu, D. G. (2011). A venomous arthropod in the Early Cambrian Sea. *Chin. Sci. Bull.* 56, 1532–1534. doi: 10.1007/s11434-011-4371-6

Fusco, G., and Minelli, A. (2010). Phenotypic plasticity in development and evolution: facts and concepts. *Philos. Trans. R. Soc. B.: Biol. Sci.* 365, 547–556. doi: 10.1098/rstb.2009.0267

Giribet, G., and Edgecombe, G. D. (2019). The phylogeny and evolutionary history of arthropods. *Curr. Biol.* 29, R592–R602. doi: 10.1016/j.cub.2019.04.057

Hammer, O. (2001). PAST: Paleontological statistics software package for education and data analysis. *Palaeontol. Electron.* 4, 9.

Hopkins, M. J., and Webster, M. (2009). Ontogeny and geographic variation of a new species of the corynexochine trilobite Zacanthopsis (Dyeran, Cambrian). *J. Paleontol.* 83, 524–547. doi: 10.1666/08-102R.1

Hou, X. G., Aldridge, R. J., Bergström, J., Siveter, D. J., Siveter, D. J., and Feng, X. H. (2004). *The Cambrian fossils of Chengjiang, China: the flowering of early animal life* Vol. 233 (Oxford: Blackwell), 1–233.

Hou, X. G., Chen, J. Y., and Lu, H. Z. (1989). Early Cambrian new arthropods from Chengjiang, Yunnan. *Acta Palaeontol. Sin.* 28, 42–57. doi: 10.19800/j.cnki.aps.1989.01.004

Hou, X. G., Siveter, D. J., Siveter, D. J., Aldridge, R. J., Cong, P. Y., Gabbott, S. E., et al. (2017). *The Cambrian fossils of Chengjiang, China: The flowering of early animal life* (Hoboken, NJ: John Wiley & Sons). doi: 10.1002/9781118896372

Hou, X. G., and Strom, J. B. (1997). "Arthropods of the lower Cambrian Chengjiang fauna, southwest China," in *Arthropods of the Lower Cambrian Chengjiang fauna, southwest China*. Copenhagen: Fossils and Strata, 1–117. doi: 10.18261/8200376931-1997-01

Hu, C. H. (1971). Ontogeny and sexual dimorphism of lower Paleozoic Trilobita. *Palaeontogr. Am.* 7, 31–155.

Hughes, N. C., and Fortey, R. A. (1995). Sexual dimorphism in trilobites, with an Ordovician case study. In Ordovician Odyssey: Short papers for the Seventh International Symposium on the Ordovician System, SEPM book, 77, 419–422.

Hughes, N. C., and Labandeira, C. C. (1995). The stability of species in taxonomy. *Paleobiology* 21, 401–403. doi: 10.1017/S0094837300013440

Hughes, N. C., Minelli, A., and Fusco, G. (2006). The ontogeny of trilobite segmentation: a comparative approach. *Paleobiology* 32, 602–627. doi: 10.1666/06017.1

Hultgren, K. M., and Stachowicz, J. J. (2009). Evolution of decoration in majoid crabs: a comparative phylogenetic analysis of the role of body size and alternative defensive strategies. *Am. Nat.* 173, 566–578. doi: 10.1086/597797

Jackson, I. S., and Budd, G. E. (2017). Intraspecific morphological variation of Agnostus pisiformis, a Cambrian Series 3 trilobite-like arthropod. *Lethaia* 50, 467–485. doi: 10.1111/let.12201

Knell, R. J., and Fortey, R. A. (2005). Trilobite spines and beetle horns: sexual selection in the Palaeozoic? *Biol. Lett.* 1, 196–199. doi: 10.1098/rsbl.2005.0304

Labandeira, C. C., and Hughes, N. C. (1994). Biometry of the Late Cambrian trilobite genus Dikelocephalus and its implications for trilobite systematics. *J. Paleontol.* 68, 492–517. doi: 10.1017/S0022336000025889

Lei, Q. P., Liu, Q., and Peng, S. C. (2023). Three species of Pagodia (Corynexochida, Trilobita) from the Furongian (Cambrian) of northern Anhui, China and their intraspecific variation. *Palaeoworld* 32, 27–43. doi: 10.1016/j.palwor.2022.07.002

Lerosey-Aubril, R., Kimmig, J., Pates, S., Skabelund, J., Weug, A., and Ortega-Hernández, J. (2020). New exceptionally preserved panarthropods from the Drumian Wheeler Konservat-Lagerstätte of the House Range of Utah. *Papers. Palaeontol.* 6, 501–531. doi: 10.1002/spp2.1307

Lerosey-Aubril, R., and Ortega-Hernández, J. (2019). Appendicular anatomy of the artiopod Emeraldella brutoni from the middle Cambrian (Drumian) of western Utah. *PeerJ* 7, e7945. doi: 10.7717/peerj.7945

Losso, S. R., and Ortega-Hernández, J. (2022). Claspers in the mid-Cambrian *Olenoides serratus* indicate horseshoe crab–like mating in trilobites. *Geology* 50, 897–901. doi: 10.1130/G49872.1

Luo, H. L., Hu, S. X., Zhang, S. H., and Tao, Y. H. (1997). New occurrence of the Early Cambrian Chengjiang fauna in Haikou, Kunming, Yunnan province, and study on trilobitoidea. *Acta Geol. Sin. - English. Edition.* 71, 122–132. doi: 10.1111/j.1755-6724.1997.tb00352.x

Ma, J. X., Pates, S., Wu, Y., Lin, W. L., Liu, C., Wu, Y. H., et al. (2023). Ontogeny and brooding strategy of the early Cambrian arthropod Isoxys minor from the Qingjiang biota. *Front. Ecol. Evol.* 11. doi: 10.3389/fevo.2023.1174564/full

Mayers, B., Aria, C., and Caron, J. B. (2019). Three new naraoiid species from the Burgess Shale, with a morphometric and phylogenetic reinvestigation of Naraoiidae. *Palaeontology* 62, 19–50. doi: 10.1111/pala.12383

Minelli, A., and Fusco, G. (2013). *Arthropod post-embryonic development. In Arthropod biology and evolution: molecules, development, morphology* (Berlin, Heidelberg: Springer Berlin Heidelberg), 91–122. doi: 10.1007/978-3-642-36160-9_5

Ortega-Hernández, J., Legg, D. A., and Braddy, S. J. (2013). The phylogeny of aglaspidid arthropods and the internal relationships within Artiopoda. *Cladistics* 29, 15–45. doi: 10.1111/j.1096-0031.2012.00413.x

Owen, R. (1852). Description of the impressions and foot-prints of the Protichnites from the Potsdam Sandstone of Canada. *Q. J. Geol. Soc.* 8 (1–2), 214–225. doi: 10.1144/GSL.JGS.1852.008.0102.26

Paterson, J. R., García-Bellido, D. C., and Edgecombe, G. D. (2012). New artiopodan arthropods from the early Cambrian Emu Bay Shale Konservat-Lagerstätte of South Australia. *J. Paleontol.* 86, 340–357. doi: 10.1666/11-077.1

Requieron, E. A., Torres, M. A. J., and Demayo, C. G. (2012). Applications of relative warp analysis in describing of scale shape morphology between sexes of the snakehead fish Channa striata. *Int. J. Biol. Ecol. Environ. Sci.* 1, 205–209.

Rohlf, F. J. (1993). Relative warp analysis and an example of its application to mosquito wings. *Contributions. to Morphometrics.* 8, 131–159.

Rohlf, F. J. (2010). *TPSDig2 version 2.16* (Stony Brook, NY: Department of Ecology and Evolution, State University of New York).

Saleh, F., Qi, C., Buatois, L. A., Mángano, M. G., Paz, M., Vaucher, R., et al. (2022). The Chengjiang Biota inhabited a deltaic environment. *Nat. Commun.* 13, 1569. doi: 10.1038/s41467-022-29246-z

Schmidt, M., Hou, X. G., Zhai, D. Y., Mai, H. J., Belojević, J., Chen, X. H., et al. (2022). Before trilobite legs: Pygmaclypeatus daziensis reconsidered and the ancestral appendicular organization of Cambrian artiopods. *Philos. Trans. R. Soc. B.* 377, 20210030. doi: 10.1098/rstb.2021.0030

Smith, J. M. (1998). *Evolutionary Genetics* (Oxford, UK: Oxford University Press), 273–274.

Stein, M. (2011). A new look at old data; an example from the arthropods. *Palaios* 26, 391–393. doi: 10.2110/palo.2011.S04

Stein, M., Budd, G. E., Peel, J. S., and Harper, D. A. (2013). Arthroaspisn. gen., a common element of the Sirius Passet Lagerstätte (Cambrian, North Greenland), sheds light on trilobite ancestry. *BMC Evol. Biol.* 13, 1–34. doi: 10.1186/1471-2148-13-99

Stein, M., and Selden, P. A. (2012). A restudy of the Burgess Shale (Cambrian) arthropod Emeraldella brocki and reassessment of its affinities. *J. Syst. Palaeontol.* 10, 361–383. doi: 10.1080/14772019.2011.566634

Team, P. I., Berné, O., Habart, É., Peeters, E., Abergel, A., Bergin, E. A., et al. (2022). PDRs4All: A JWST early release science program on radiative feedback from massive stars. *Publications. Astronomical. Soc. Pac.* 134, 054301. doi: 10.1088/1538-3873/ac604c/meta

Vannier, J., Caron, J. B., Yuan, J. L., Briggs, D. E., Collins, D., Zhao, Y. L., et al. (2007). Tuzoia: morphology and lifestyle of a large bivalved arthropod of the Cambrian seas. *J. Paleontol.* 81, 445–471. doi: 10.1666/05070.1

Vannier, J., and Chen, J. Y. (2000). The Early Cambrian colonization of pelagic niches exemplified by Isoxys (Arthropoda). *Lethaia* 33, 295–311. doi: 10.1080/00241160750053862

Zhang, M. Y., Liu, Y., Hou, X. G., Ortega-Hernández, J., Mai, H. J., Schmidt, M., et al. (2022). Ventral morphology of the non-trilobite artiopod retifacies abnormalis Hou, Chen & Lu 1989, from the early Cambrian Chengjiang Biota, China. *Biology* 11, 1235. doi: 10.3390/biology11081235

Zhang, X. L., Liu, W., and Zhao, Y. L. (2008). Cambrian Burgess Shale-type Lagerstätten in south China: distribution and significance. *Gondwana. Res.* 14, 255–262. doi: 10.1016/j.gr.2007.06.008

Zhang, X. L., Shu, D. G., Li, Y., and Han, J. (2001). New sites of Chengjiang fossils: crucial windows on the Cambrian explosion. *J. Geol. Soc.* 158, 211–218. doi: 10.1144/jgs.158.2.21

Zhang, X. L., Han, J., and Shu, D. G. (2000). A new arthropod Pygmaclypeatus daziensis from the early Cambrian Chengjiang Lagerstätte, South China. *J. Paleontol.* 74 (5), 979–982. doi: 10.1666/00223360(2000)074<0979:ANAPDF>2.0.CO;2

Zhao, F. C., Zhu, M. Y., and Hu, S. X. (2010). Community structure and composition of the Cambrian Chengjiang biota. *Sci. China Earth Sci.* 53, 1784–1799. doi: 10.1007/s11430-010-4087-8

Zhu, Y. Y., Zeng, H., Liu, Y., and Zhao, F. C. (2023). New artiopodan euarthropods from the Chengjiang fauna (Cambrian, Stage 3) at Malong, Yunnan, China. *Acta Palaeontol. Polonica.* 68, 427–440. doi: 10.4202/app.01080.2023